Chemical Engineering Communications

ISSN: 0098-6445 (Print) 1563-5201 (Online) Journal homepage: https://www.tandfonline.com/loi/gcec20

TWO-DIMENSIONAL SOLUTION AND ANALYSIS OF A CYLINDRICAL MATRIX DEVICE WITH A CIRCULAR RELEASE AREA

Laurent Simon & Juan Ospina

To cite this article: Laurent Simon & Juan Ospina (2013) TWO-DIMENSIONAL SOLUTION AND ANALYSIS OF A CYLINDRICAL MATRIX DEVICE WITH A CIRCULAR RELEASE AREA, Chemical Engineering Communications, 200:1, 115-138, DOI: 10.1080/00986445.2012.695302

To link to this article: https://doi.org/10.1080/00986445.2012.695302

Chem. Eng. Comm., 200:115–138, 2013

ISSN: 0098-6445 print/1563-5201 online
DOI: 10.1080/00986445.2012.695302

Taylor & Francis
Taylor & Francis Group

Two-Dimensional Solution and Analysis of a Cylindrical Matrix Device with a Circular Release Area

LAURENT SIMON[1] AND JUAN OSPINA[2]

[1]Otto H. York Department of Chemical, Biological and Pharmaceutical Engineering, New Jersey Institute of Technology, Newark, New Jersey, USA
[2]Logic and Computation Group, Physics Engineering Program, School of Sciences and Humanities, EAFIT University, Medellin, Colombia

A cylindrical device was analyzed using a Laplace transform–based method. The two-dimensional model represented a pharmaceutical agent uniformly distributed in a polymeric matrix surrounded by an impermeable layer. Molecules could be transferred only through a small hole centered at the top surface of the cylinder. A closed-form solution was obtained to help study the effects of design parameters and geometries on the cumulative amount of drug released. The latter variable increased with the mass transfer and diffusion coefficients and decreased with any increment in the device's length. The delivery rate was described by an effective time constant calculated from Laplace transforms. Reducing the orifice diameter or fabricating a longer system would delay transport of the medication. Simplified expressions for the release profile and the time constant were derived for special design cases.

Keywords Controlled release; Diffusion; Drug delivery; Effective time constant; Mathematical modeling; Simulation; Transport phenomena

Introduction

Controlled-release formulations are found in several applications. Transdermal patches are manufactured to deliver nitroglycerin and provide relief against episodes of angina (Wang et al., 1998). Opiods, such as buprenorphine and fentanyl, can be administered through the skin for the treatment of chronic pain (Andresen et al., 2011). The notion of releasing a desired rate of an active pharmaceutical ingredient (API) in a controlled and virtually painless manner has attracted many researchers, who are now finding novel uses for the technology. DentiPatch (Noven Pharmaceuticals) is a small patch that is placed against the gum line to deliver lidocaine (Leopold et al., 2002). Actiq is a product that provides oral transmucosal delivery

Address correspondence to Laurent Simon, Otto H. York Department of Chemical, Biological and Pharmaceutical Engineering, New Jersey Institute of Technology, Newark, NJ 07102, USA. E-mail: laurent.simon@njit.edu

of fentanyl citrate (Mystakidou et al., 2007). Drug-eluting stents, composed of a biodegradable polymer containing a drug, have been studied for long-term delivery of paclitaxel and rapamycin in an effort to prevent restenosis (Alexis et al., 2004). This condition is characterized by a re-blockage of the blood vessels after implanting a stent.

The physical shape of the drug-delivery system is a critical factor that is determined, in part, by the intended location of the device and its ultimate application. Flat membranes are affixed to the skin surface, while conical dissolving microneedles are fabricated to penetrate the stratum corneum. Cylindrical matrices remain very popular and are being used in technologies ranging from oral delivery (Rosca and Vergnaud, 2008) to implants (Qian et al., 2001). Punctal plugs are designed for the ophthalmic uptake of cyclosporine A to help patients with dry-eye syndrome (Gupta and Chauhan, 2001). Compressed lipid implants have been studied for their potential roles in releasing acid-labile drugs (Kreye et al., 2001). The shell protects the drug from being released into the gastric fluid. A design, first proposed by Tojo and Miyanami for prolonged drug release, is considered in this work (Tojo and Miyanami, 1983; Tojo, 1984). A monolithic system is devised for the release of an API (Figure 1). The product is coated so that there is no mass exchange with the environment except for a small release hole pierced in the top of the cylinder. This technology is of interest because several studies have proposed cylinder-with-opening type designs to obtain a desired delivery rate (Ertan et al., 1997, 2005; Hsu et al.,

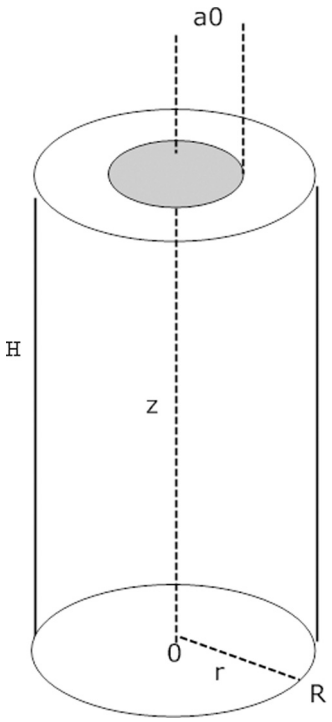

Figure 1. Diagram of the cylindrical controlled-release device (adapted from Figure 2 of Tojo and Miyanami (1983) and Figure 1 in Tojo (1984)).

1992). The approach adopted in this contribution may be applied to investigate such devices and improve their performances.

A two-dimensional model was formulated by Tojo and Miyanami (1983). In the original article, a numerical procedure was implemented to study the effects of design specifications (e.g., height, diameters) on the cumulative amount of drug released. An analytical solution was available only for cases when the diameter of the hole was equal to that of the monolithic model. In addition, the derivation of a single effective time constant to estimate the release rate was not presented. Such a parameter would allow drug manufacturers to fabricate delivery systems that meet a specified dynamic performance criterion. The goal of this project is to develop an evaluation platform to facilitate the analysis of drug release from cylindrical matrix devices. Design considerations, such as dimensions of the system and properties of the polymer, can be assessed with a minimum number of experiments.

This article is arranged as follow. An analytical solution is derived for the model originally proposed by Tojo and Miyanami (1983). Laplace transform techniques, with Bromwich integral and the residue theorem, are applied. Maple (Waterloo Software Inc.) routines are coded to implement the methodology and generate the simulations. A closed-form expression for the ratio $M(t)/M(\infty)$ is developed, where M(t) is the cumulative amount of the active agent released at time t and $M(\infty)$ is the mass initially loaded into the device. The rate at which $M(t)/M(\infty)$ approaches 1 is calculated using a method proposed in the literature (Simon, 2011). The effects of the geometry and transport parameters on performance are given in the Results and Discussions section. Comparisons with published results are presented.

Materials and Methods

Mathematical Modeling

The system studied is a cylindrical monolithic structure inside of which an active agent, A, is dissolved or dispersed uniformly (Tojo and Miyanami, 1983). The matrix is coated with an impermeable substance. The drug is released through a small circular hole drilled in the center of the top surface (Figure 1). A balance on component A gives

$$\frac{\partial}{\partial t}C_A(t,r,z) = \frac{\eta_A\left(\left(\frac{\partial}{\partial r}C_A(t,r,z)\right) + r\left(\frac{\partial^2}{\partial r^2}C_A(t,r,z)\right)\right)}{r} + \eta_A\left(\frac{\partial^2}{\partial z^2}C_A(t,r,z)\right) \quad (1)$$

where $C_A(t,r,z)$ denotes the concentration of A located at the point (r,z) and η_A is the drug diffusion coefficient in the matrix.

The initial condition for (1) is

$$C_A(0,r,z) = c_{AS}, 0 < r < R, \quad 0 < z < H \quad (2)$$

where c_{AS} is the saturated concentration of A in the matrix. The boundary conditions are (Tojo and Miyanami, 1983)

$$\left(\frac{\partial}{\partial r}C_A(t,r,z)\right)\Big|_{r=R} = 0, \ t > 0, \ 0 < z < H \quad (3)$$

$$\left(\frac{\partial}{\partial z}C_A(t,r,z)\right)\Big|_{z=0} = 0,\ t>0,\ 0<r<R \tag{4}$$

$$\left(\frac{\partial}{\partial z}C_A(t,r,z)\right)\Big|_{z=H} = \begin{cases} -\frac{k_m\, C_A(t,r,H)}{\eta_A} & r \le a_0 \\ 0 & a_0 < r \end{cases} \tag{5}$$

These boundary conditions, Equations (3)–(5), correspond to the previously described situation where the drug is released only through the small circular hole of radius a_0 drilled at $z=H$. The parameter k_m is a boundary-layer mass transfer coefficient. A high k_m is indicative of a low mass transfer resistance due to factors, such as vigorous mixing, that can reduce the thickness of the layer. Low k_m values would decrease the rate at which drugs leave the small orifice.

Equations (1)–(5) can be written in the following dimensionless form (Tojo and Miyanami, 1983):

$$\frac{\partial}{\partial\tau}\mathrm{C}(\tau,\,\rho,\zeta) = \frac{\frac{\partial}{\partial\rho}\mathrm{C}(\tau,\,\rho,\zeta)}{\rho} + \left(\frac{\partial^2}{\partial\rho^2}\mathrm{C}(\tau,\,\rho,\zeta)\right) + \left(\frac{\partial^2}{\partial\zeta^2}\mathrm{C}(\tau,\,\rho,\,\zeta)\right) \tag{6}$$

$$\mathrm{C}(0,\rho,\zeta) = 1,\ 0<\rho<1,\ 0<\zeta<\frac{\mathrm{H}}{\mathrm{R}} \tag{7}$$

$$\left(\frac{\partial}{\partial\rho}\mathrm{C}(\tau,\rho,\zeta)\right)\Big|_{\rho=1} = 0,\ \tau>0,\ 0<\zeta<\frac{\mathrm{H}}{\mathrm{R}} \tag{8}$$

$$\left(\frac{\partial}{\partial\zeta}\mathrm{C}(\tau,\rho,\zeta)\right)\Big|_{\zeta=0} = 0,\ \tau>0,\ 0<\rho<1 \tag{9}$$

$$\left(\frac{\partial^2}{\partial\zeta^2}\mathrm{C}(\tau,\,\rho,\zeta)\right)\Big|_{\zeta=\frac{H}{R}} = \begin{cases} -Sh\ \mathrm{C}\left(\tau,\rho,\frac{H}{R}\right) & \rho \le \frac{a_0}{R} \\ 0 & \frac{a_0}{R} < \rho \end{cases} \tag{10}$$

The dimensionless magnitudes appearing in Equation (6–10) are defined as follows:

$$\rho = \frac{r}{R},\quad \zeta = \frac{z}{R},\quad \tau = \frac{t\,\eta_{\mathrm{A}}}{R^2},\quad \mathrm{C}(\tau,\rho,\zeta) = \frac{C_A(\tau,\rho,\zeta)}{c_{AS}},\quad Sh = \frac{R\,k_m}{\eta_{\mathrm{A}}} \tag{11}$$

The Sherwood number Sh is a dimensionless number that represents the ratio of convective to diffusive mass transfer. This parameter is directly proportional to k_m and inversely proportional to η_{A}.

Analytical Solution

The analytical solution to the dimensionless problem, Equations (6)–(10), can be derived using the Laplace transform technique with the Bromwich integral and the residue theorem. The procedure is implemented in Maple. Taking the Laplace

transform of Equation (6) gives

$$s\overline{C}(s,\rho,\zeta) - 1 = \frac{\frac{\partial \overline{C}(s,\rho,\zeta)}{\partial \rho}}{\rho} + \frac{\partial^2}{\partial \rho^2}\overline{C}(s,\rho,\zeta) + \frac{\partial^2}{\partial \zeta^2}\overline{C}(s,\rho,\zeta) \tag{12}$$

after using the initial condition. The general solution of Equation (12) is (using Maple's PDEtools package):

$$\begin{aligned}\overline{C}(s,\rho,\zeta) = &\left[C_1 \sin\left(\sqrt{-s+c_1}\zeta\right) + C_2 \cos\left(\sqrt{-s+c_1}\zeta\right)\right] \\ &\left[C_3 J_0\left(\sqrt{-c_1}\rho\right) + C_4 Y_0\left(\sqrt{-c_1}\rho\right)\right] + \frac{1}{s}\end{aligned} \tag{13}$$

where J_0 and Y_0 are Bessel functions of the first kind and second kind, respectively, and C_1, C_2, C_3, C_4, and c_1 are constants to be determined using the boundary conditions. Because Y_0(x) is singular at x = 0, the constant C_4 should be zero for a finite solution at $\rho = 0$. Equation (13) becomes

$$\overline{C}(s,\rho,\zeta) = \left[C_1 \sin\left(\sqrt{-s+c_1}\zeta\right) + C_2 \cos\left(\sqrt{-s+c_1}\zeta\right)\right] C_3 J_0\left(\sqrt{-c_1}\rho\right) + \frac{1}{s} \tag{14}$$

Without any lost of generality, C_3 is set equal to 1, which yields

$$\overline{C}(s,\rho,\zeta) = \left[C_1 \sin\left(\sqrt{-s+c_1}\zeta\right) + C_2 \cos\left(\sqrt{-s+c_1}\zeta\right)\right] J_0\left(\sqrt{-c_1}\rho\right) + \frac{1}{s} \tag{15}$$

After applying Equation (9), Equation (15) gives $J_0\left(\sqrt{-c_1}\,\rho\right)\sqrt{-s+c_1}C_1 = 0$, implying that $C_1 = 0$. As a result

$$\overline{C}(s,\rho,\zeta) = C_2 \cos\left(\sqrt{-s+c_1}\zeta\right) J_0\left(\sqrt{-c_1}\rho\right) + \frac{1}{s} \tag{16}$$

The use of Equation (8) leads to

$$-C_2 \cos\left(\sqrt{-s+c_1}\,\zeta\right) J_1\left(\sqrt{-c_1}\right)\sqrt{-c_1} = 0 \tag{17}$$

Consequently, $J_1\left(\sqrt{-c_1}\right) = 0$, which admits an infinite number of real roots: $\sqrt{-c_1} = \alpha_{1,n}$ or $c_1 = -\alpha_{1,n}^2$. Equation (16) becomes

$$\overline{C}(s,\rho,\zeta) = C_2 \cos\left(\sqrt{-s-\alpha_{1,n}^2}\zeta\right) J_0\left(\alpha_{1,n}\rho\right) + \frac{1}{s} \tag{18}$$

where n is an integer from 0 to ∞. Application of the superposition principle results in

$$\overline{C}(s,\rho,\zeta) = \sum_{n=0}^{\infty}\left[F_n \cos\left(\sqrt{-s-\alpha_{1,n}^2}\zeta\right) J_0\left(\alpha_{1,n}\rho\right)\right] + \frac{1}{s} \tag{19}$$

which can be rewritten as

$$\overline{C}(s,\rho,\zeta) = F_0 \cos\left(\sqrt{-s-\alpha_{1,0}^2}\zeta\right) J_0\left(\alpha_{1,0}\rho\right) + \sum_{n=1}^{\infty}\left[F_n \cos\left(\sqrt{-s-\alpha_{1,n}^2}\zeta\right) J_0\left(\alpha_{1,n}\rho\right)\right] + \frac{1}{s} \tag{20}$$

or

$$\overline{C}(s,\rho,\zeta) = F_0 \cos\left(\sqrt{-s}\zeta\right) + \sum_{n=1}^{\infty}\left[F_n \cos\left(\sqrt{-s-\alpha_{1,n}^2}\zeta\right) J_0\left(\alpha_{1,n}\rho\right)\right] + \frac{1}{s} \tag{21}$$

since $\alpha_{1,0}=0$. Applying the boundary condition given by Equation (10) to Equation (21), the following equality is obtained:

$$-F_0\sqrt{-s}\sin\left(\sqrt{-s}\frac{H}{R}\right) + \sum_{n=1}^{\infty}\left[-F_n\sqrt{-s-\alpha_{1,n}{}^2}\sin\left(\sqrt{-s-\alpha_{1,n}{}^2}\frac{H}{R}\right) J_0(\alpha_{1,n}\rho)\right] = \begin{cases} -Sh\left\{F_0\cos\left(\sqrt{-s}\frac{H}{R}\right) + \sum_{n=1}^{\infty}\left[F_n\cos\left(\sqrt{-s-\alpha_{1,n}{}^2}\frac{H}{R}\right) J_0\left(\alpha_{1,n}\rho\right)\right] + \frac{1}{s}\right\}; & \rho \le \frac{a_0}{R} \\ 0; & \frac{a_0}{R} < \rho \end{cases} \tag{22}$$

Multiplying both sides of Equation (22) by ρ and integrating the results from 0 to 1 leads to

$$F_0 = \frac{Sh\, a_0\left(2\left(\sum_{n=1}^{\infty}\frac{F_n\cos\left(\frac{\sqrt{-s-\alpha_{1,n}^2}H}{R}\right) J_1\left(\frac{\alpha_{1,n}a_0}{R}\right)}{\alpha_{1,n}}\right) s\,R + a_0\right)}{s\left(\sin\left(\frac{\sqrt{-s}H}{R}\right)\sqrt{-s}\,R^2 - Sh\,\cos\left(\frac{\sqrt{-s}H}{R}\right) a_0^2\right)} \tag{23}$$

On the other hand, multiplying both sides of Equation (22) by $\rho J_0(\alpha_{1,\,p}\rho)$ and integrating the results from 0 to 1 lead to the following system composed of an infinite number of equations:

$$\begin{aligned} &-\frac{1}{2}F_p\sin\left(\sqrt{-s-\alpha_{1,p}^2}\frac{H}{R}\right)\sqrt{-s-\alpha_{1,p}^2}J_0\left(\alpha_{1,p}\right)^2 = \\ &-\frac{ShF_0\cos\left(\sqrt{-s}\frac{H}{R}\right)a_0 J_1\left(\frac{\alpha_{1,p}a_0}{R}\right)}{\alpha_{1,p}R} \\ &+\sum_{n=1}^{\infty}\left[-ShF_n\cos\left(\sqrt{-s-\alpha_{1,n}^2}\frac{H}{R}\right)\int_0^{\frac{a_0}{R}} J_0\left(\alpha_{1,n}\rho\right)\rho J_0\left(\alpha_{1,p}\rho\right)d\rho\right] \\ &-\frac{Sha_0 J_1\left(\frac{\alpha_{1,p}a_0}{R}\right)}{s\alpha_{1,p}R} \end{aligned} \tag{24}$$

which can be solved for F_n when Equation (23) is replaced in Equation (24). The subscript p is an integer that varies from 1 to ∞. Expressions for F_0 and the first M F_i coefficients (i.e., $i = 1, \ldots M$) can be replaced in Equation (21) to yield the transform $\overline{C}(s, \rho, \zeta)$. The parameter M is selected to achieve a desired degree of accuracy. A formal expression for the dimensionless concentration in the time domain can be derived by taking the inverse Laplace transform of $\overline{C}(s, \rho, \zeta)$ using the Bromwich integral and the residue theorem.

If F_n is replaced by the quotient $P_{\mathrm{n}}(\mathrm{s})/Q_{\mathrm{n}}(\mathrm{s})$, we have

$$\begin{aligned}\overline{C}(s,\rho,\zeta) = & \\ & -\frac{Sh\,a_0\left(2\left(\sum_{n=1}^{\infty}\frac{P_n(s)\cos\left(\frac{\sqrt{-s-\alpha_{1,n}^2}\,H}{R}\right)J_1\left(\frac{\alpha_{1,n}a_0}{R}\right)}{Q_n(s)\,\alpha_{1,n}}\right)sR+a_0\right)\cos(\sqrt{-s}\,\zeta)}{s\left(-\sin\left(\frac{\sqrt{-s}\,H}{R}\right)\sqrt{-s}\,R^2-Sh\cos\left(\frac{\sqrt{-s}\,H}{R}\right)a_0^2\right)} \\ & +\left(\sum_{n=1}^{\infty}\frac{J_0(\alpha_{1,n}\rho)P_n(s)\cos\sqrt{-s-\alpha_{1,n}^2}\,\zeta}{Q_n(s)}\right)+\frac{1}{s}\end{aligned} \tag{25}$$

which can be rewritten as

$$\begin{aligned}\overline{C}(s,\rho,\zeta) = & -\frac{2a_0\,Sh\left\{\sum_{n=1}^{\infty}\left[\frac{P_n(s)\cos\left(\frac{\sqrt{-s-\alpha_{1,n}^2}\,H}{R}\right)J_1\left(\frac{\alpha_{1,n}a_0}{R}\right)}{Q_n(s)\alpha_{1,n}}\right]\right\}R\cos(\sqrt{-s}\zeta)}{-\sin\left(\frac{\sqrt{-s}H}{R}\right)\sqrt{-s}R^2+Sh\cos\left(\frac{\sqrt{-s}H}{R}\right)a_0^2} \\ & -\frac{a_0^2Sh\cos(\sqrt{-s}\zeta)}{s\left[-\sin\left(\frac{\sqrt{-s}H}{R}\right)\sqrt{-s}R^2+Sh\cos\left(\frac{\sqrt{-s}H}{R}\right)a_0^2\right]} \\ & +\left\{\sum_{n=1}^{\infty}\left[\frac{J_0\left(\alpha_{1,n}\rho\right)P_n(s)\cos\left(\sqrt{-s-\alpha_{1,n}^2}\zeta\right)}{Q_n(s)}\right]\right\}+\frac{1}{s}\end{aligned} \tag{26}$$

The inverse Laplace transform of Equation (26) is given by

$$C(\tau,\rho,\zeta) = C_1(\tau,\,\rho,\,\zeta) + C_2(\tau,\,\rho,\,\zeta) + C_3(\tau,\,\rho,\,\zeta) + C_4(\tau,\,\rho,\,\zeta) \tag{27}$$

where

$$C_1(\tau,\rho,\zeta) = \sum_{p=1}^{\infty}\left(\begin{array}{l}-\frac{4Sh^2a_0^3R^3\cos\left(\frac{\beta_pR\zeta}{H}\right)e^{\left(-\frac{\beta_p^2R^2\tau}{H^2}\right)}\beta_p}{\sin\left(\beta_p\right)\left(R^3HSha_0^2+\beta_p^2R^6+Sh^2H^2a_0^4\right)}\times \\ \sum_{n=1}^{\infty}\frac{P_n\left(-\frac{\beta_p^2R^2}{H^2}\right)\cosh\left(\frac{\sqrt{\alpha_{1,n}^2H^2-\beta_p^2R^2}}{R}\right)J_1\left(\frac{\alpha_{1,n}a_0}{R}\right)}{Q_n\left(-\frac{\beta_p^2R^2}{H^2}\right)\alpha_{1,n}}\end{array}\right) \tag{28}$$

$$C_2(\tau,\rho,\zeta)=\sum_{q=1}^{\infty}\left(\begin{array}{l}-\frac{2a_0 ShR\cos(\sqrt{-s}\zeta)e^{s\tau}}{-\sin\left(\frac{\sqrt{-s}H}{R}\right)\sqrt{-s}R^2+Sh\cos\left(\frac{\sqrt{-s}H}{R}\right)a_0^2}\times \\ \sum_{n=1}^{\infty}\left[\frac{P_n(s)\cos\left(\frac{\sqrt{-s-\alpha_{1,n}^2}H}{R}\right)J_1\left(\frac{\alpha_{1,n}a_0}{R}\right)}{\frac{dQ_n(s)}{ds}\alpha_{1,n}}\right]\end{array}\right)\Bigg|_{s=S_q} \tag{29}$$

$$C_3(\tau,\ \rho,\ \zeta)=\sum_{p=1}^{\infty}\left(\frac{2\,Sh^2\,a_0^4\cos\left(\frac{\beta_p R\zeta}{H}\right)e^{\left(\frac{\beta_p^2R^2\tau}{H^2}\right)}H^2}{\beta_p\,\sin(\beta_p)(R^3H\,Sh\,a_0^2+\beta_p^2R^6+Sh^2\,H^2\,a_0^4)}\right) \tag{30}$$

$$C_4(\tau,\rho,\zeta)=\sum_{n=1}^{\infty}\left(\sum_{q=1}^{\infty}\frac{J_0(\alpha_{1,n}\rho)P_n(s)\ \cos\left(\sqrt{-s-\alpha_{1,n}^2}\,\zeta\right)\mathrm{e}^{(s\tau)}}{\frac{d}{ds}Q_n(s)}\Bigg|_{s=S_q}\right) \tag{31}$$

The parameters β_{p} are the solutions of the equation

$$\cos(\beta_p)=\frac{\sin(\beta_p)\,\beta_p\,R^3}{H\,Sh\,a_0^2} \tag{32}$$

and S_{q} represent the roots of the equation $Q_n(s)=0$. Algorithms are coded in Maple to simulate the drug concentration (Equation (27)).

Time Constant for the Cumulative Percentage of Drug Released

From the concentration $C_A(t, r, z)$, it is possible to derive the time it takes to release the total amount of the active agent initially dissolved in the matrix. The method proposed by Simon is applied (Simon, 2011). By definition, the cumulative amount of the active agent released into the environment at time t, denoted $M(t)$, is the difference between the amount of A initially dissolved in the polymeric matrix and the amount of A remaining at time t (Tojo and Miyanami, 1983):

$$\mathrm{M}(t)=c_{AS}\,\pi\,R^2\,H-2\pi\int_0^H\int_0^R C_A(t,r,z)r\,dr\,dz \tag{33}$$

Equation (33) is rewritten, in terms of dimensionless variables, as

$$\mathrm{M}(\tau)=c_{AS}\,\pi\,R^2\,H-2\pi\,R^3\,c_{AS}\int_0^{\frac{H}{R}}\int_0^1\mathrm{C}\,(\tau,\ \rho,\ \zeta)\rho\,d\rho\,d\zeta \tag{34}$$

The normalized form of Equation (34) is

$$\frac{\mathrm{M}(\tau)}{\mathrm{M}(\infty)}=1-\left(\frac{2R}{H}\int_0^{\frac{H}{R}}\int_0^1 C(\tau,\rho,\varsigma)\rho d\rho d\varsigma\right) \tag{35}$$

where $M(\infty) = c_{AS}\pi R^2 H$. The Laplace transform of Equation (35) is

$$\frac{M(s)}{M(\infty)} = \frac{1}{s} - \frac{2R}{H}\int_0^{\frac{H}{R}}\int_0^1 \overline{C}(s,\rho,\varsigma)\rho d\rho d\varsigma \tag{36}$$

or

$$\frac{M(s)}{M(\infty)} = \frac{1}{s} - \frac{2R}{H}\int_0^{\frac{H}{R}}\int_0^1 \left[F_0\cos\left(\sqrt{-s}\zeta\right) + \sum_{n=1}^{\infty}\left[F_n\cos\left(\sqrt{-s-\alpha_{1,n}^2}\zeta\right)J_0\left(\alpha_{1,n}\rho\right)\right] + \frac{1}{s}\right]\rho d\ \rho d\varsigma \tag{37}$$

After computing the integrals in Equation (37), the following equation is obtained:

$$\frac{M(s)}{M(\infty)} = \frac{F_0 s\ \sin\left(\frac{\sqrt{-s}H}{R}\right)R}{H(-s)^{(3/2)}} \tag{38}$$

and finally,

$$\frac{M(s)}{M(\infty)} = -\frac{Sh\,a_0\left(2\left(\sum_{n=1}^{\infty}\frac{F_n\cos\left(\frac{\sqrt{-s-\alpha_{1,n}^2}H}{R}\right)J_1\left(\frac{\alpha_{1,n}a_0}{R}\right)}{\alpha_{1,n}}\right)sR + a_0\right)\sin\left(\frac{\sqrt{-s}H}{R}\right)R}{H(-s)^{(3/2)}\left(\sin\left(\frac{\sqrt{-s}H}{R}\right)\sqrt{-s}R^2 - Sh\cos\left(\frac{\sqrt{-s}H}{R}\right)a_0^2\right)} \tag{39}$$

According to the work by Simon (2011) and Collins (1980), the effective relaxation time is defined by

$$t_{eff} = \int_0^{\infty} t\Omega(t)dt \tag{40}$$

where the probability density function $\Omega(t)$ represents

$$\Omega(t) = \frac{(\psi_{ss} - \psi(t))}{\int_0^{\infty}(\psi_{ss} - \psi(t))dt} \tag{41}$$

Equation (40) can be written in terms of Laplace variables:

$$t_{eff} = \lim_{s\to 0}\left(\frac{\psi_{ss}}{s^2} + \frac{d\bar{\psi}(s)}{ds}\right)\left[\lim_{s\to 0}\left(\frac{\psi_{ss}}{s} - \bar{\psi}(s)\right)\right]^{-1} \tag{42}$$

where ψ_{ss} is the steady-state value and $\bar{\psi}$ is the Laplace transform of ψ. When Equation (40) is applied to Equation (39) (i.e., $\psi = M(t)/M(\infty)$), the effective time becomes

$$\tau_{eff} = -\frac{\left[\frac{\partial^2}{\partial s^2}\left(\frac{sSha_0\left(2\left(\sum_{n=1}^{\infty}\frac{Fn\cos\left(\frac{\sqrt{-s-\alpha_{1,n}^2}H}{R}\right)J_1\left(\frac{\alpha_{1,n}a_0}{R}\right)}{\alpha_{1,n}}\right)sR+a_0\right)\sin\left(\frac{\sqrt{-s}H}{R}\right)R}{H(-s)^{\frac{3}{2}}\left(\sin\left(\frac{\sqrt{-s}H}{R}\right)+\sqrt{-s}R^2-Sh\cos\left(\frac{\sqrt{-s}H}{R}\right)a_0^2\right)}\right)\right]_{s=0}}{2\left[\frac{\partial}{\partial s}\left(\frac{sSha_0\left(2\left(\sum_{n=1}^{\infty}\frac{Fn\cos\left(\frac{\sqrt{-s-\alpha_{1,n}^2}H}{R}\right)J_1\left(\frac{\alpha_{1,n}a_0}{R}\right)}{\alpha_{1,n}}\right)sR+a_0\right)\sin\left(\frac{\sqrt{-s}H}{R}\right)R}{H(-s)^{\frac{3}{2}}\left(\sin\left(\frac{\sqrt{-s}H}{R}\right)+\sqrt{-s}R^2-Sh\cos\left(\frac{\sqrt{-s}H}{R}\right)a_0^2\right)}\right)\right]_{s=0}} \quad (43)$$

Results and Discussions

When the Release Hole and the Device Have Equal Diameters ($a_0 = R$)

When $a_0 = R$, the analytical profiles are compared with the numerical results reported by Tojo and Miyanami (1983). Equations (39) and (43) are reduced to

$$\frac{\mathrm{M}(s)}{\mathrm{M}(\infty)} = -\frac{Sh\ R\ \sin\left(\frac{\sqrt{-s}\,H}{R}\right)}{H(-s)^{(3/2)}\left(\sin\left(\frac{\sqrt{-s}\,H}{R}\right)\sqrt{-s} - Sh\ \cos\left(\frac{\sqrt{-s}\,H}{R}\right)\right)} \quad (44)$$

and

$$\tau_{eff} = \frac{H^2(15\,R^2 + 10\,H\,Sh\,R + 2\,Sh^2\,H^2)}{5\,R^2\,Sh\,(3\,H\,R + Sh\,H^2)} \quad (45)$$

respectively. The effective dimensional time is

$$t_{eff} = \frac{1}{5}\frac{H(15\,\eta_A^2 + 10H\,k_m\,\eta_A + 2\,k_m^2\,H^2)}{k_m(3\,\eta_A + k_m\,H)\,\eta_A} \quad (46)$$

Applying the inverse Laplace transform to Equation (44) gives

$$\frac{\mathrm{M}(\tau)}{\mathrm{M}(\infty)} = 1 - \left(\sum_{q=1}^{\infty}\left(\frac{2\,\mathrm{e}^{\left(-\frac{\beta_q^2 R^2 \tau}{H^2}\right)}\,Sh^2\,H^2}{\beta_q^2(H\,Sh\,R + \beta_q^2\,R^2 + Sh^2\,H^2)}\right)\right) \quad (47)$$

where β_q are the roots of the following equation:

$$\beta_q\,\tan(\beta_q) = \frac{H\,Sh}{R} \quad (48)$$

Equation (47) can be written, in terms of dimensionless variables, as

$$\frac{\mathrm{M}(t)}{\mathrm{M}(\infty)} = 1 - \left(\sum_{q=1}^{\infty} \left(\frac{2\,\mathrm{e}^{\left(-\frac{\beta_q^2 R^2 \tau}{H^2}\right)} L^2}{\beta_q^2 (L + \beta_q^2 + L^2)} \right) \right) \tag{49}$$

The new dimensionless number is defined by

$$L = \frac{k_m H}{\eta_A} \tag{50}$$

As a result, Equation (48) takes the form

$$\beta_q \tan(\beta_q) = L \tag{51}$$

Equations (49)–(51) coincide with Equations (14) and (15) derived by Tojo and Miyanami (1983). Figure 2 describes the trends depicted in Figure 3 of the original article. The cumulative amount of drug released increases with the mass transfer and diffusion coefficients. As the resistance to mass transfer is lowered or Fickian transport is promoted, an increasing amount of the API is delivered. A reduction in the length of the cylinder is accompanied by a rise in $M(t)/M(\infty)$.

In terms of the dimensionless parameter L, the effective time given by Equation (26) is

$$t_{eff} = \frac{1}{5} \frac{H^2 (15 + 10\,L + 2L^2)}{\eta_A\, L\, (3 + L)} \tag{52}$$

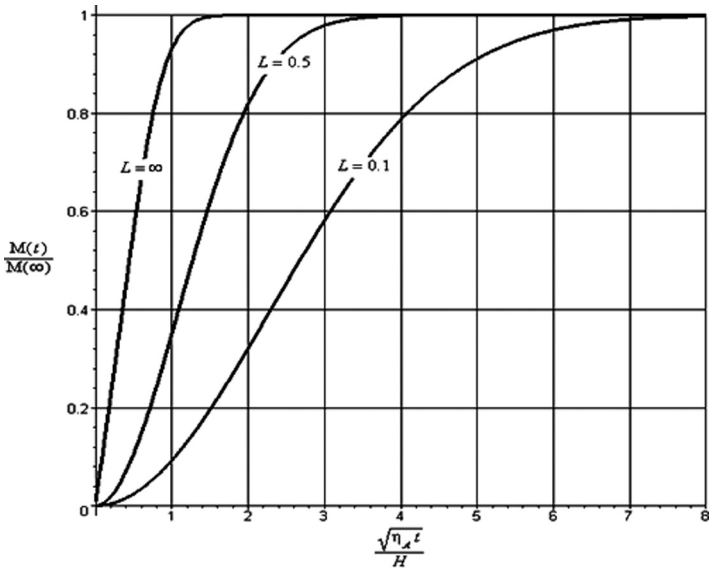

Figure 2. Influences of the parameter $L = k_m H/\eta_A$ on the cumulative amount of drug released. The profiles agree with the results reported in Figure 3 of Tojo and Miyanami (1983).

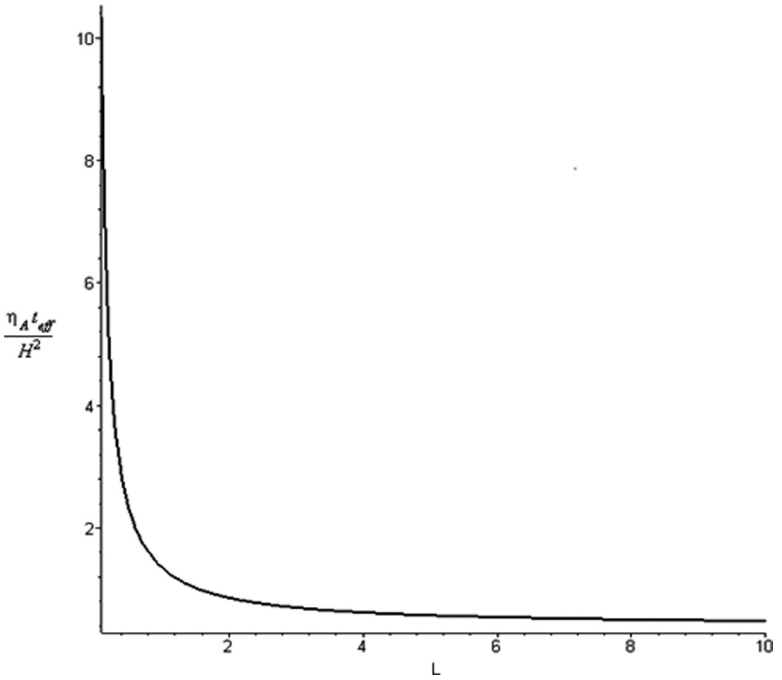

Figure 3. Effects of $L = k_m H/\eta_A$ on the effective time constant defined by Equation (52).

The variation of $\eta_A t_{eff}/H^2$ as a function of L is shown in Figure 3. The rate at which the drug is released increases with an increase in k_m. As the mass transfer boundary layer resistance becomes smaller, the drug release rate, as measured by t_{eff}, is enhanced. In particular, expressions for these limiting cases are readily computed:

$$t_{eff}(L=\infty) = \frac{2}{5}\frac{H^2}{\eta_A} \tag{53}$$

$$t_{eff}(L=0) = \infty \tag{54}$$

$$t_{eff}(L=0.1) = \frac{10.33548387\,H^2}{\eta_A} \tag{55}$$

$$t_{eff}(L=0.5) = \frac{2.342857142\,H^2}{\eta_A} \tag{56}$$

Using Equations (52) and (53), the following ratio is developed:

$$\frac{t_{eff}}{t_{eff}(L=\infty)} = \frac{15+10\,L+2\,L^2}{2\,L\,(3+L)} \tag{57}$$

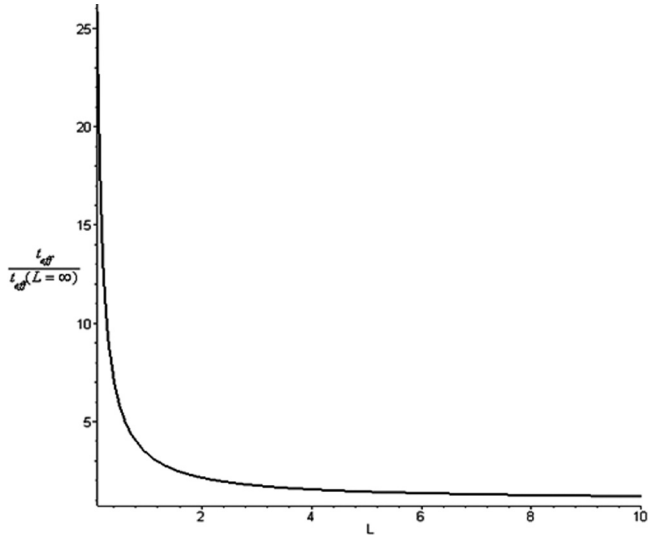

Figure 4. Impacts of $L = k_m H/\eta_A$ on the normalized effective time constant defined by Equation (57).

Equation (57) is shown in Figure 4, which may be useful for design purposes because it relates a normalized time constant to the parameter L. This information provides product manufacturers great flexibility in meeting a desired dynamic performance. Three factors, k_m, H, and η_A, can be manipulated to reach a target t_{eff}.

When the Release Hole is Slightly Smaller Than the Device ($0.9R \leq a_0 \leq R$)

When the radius of the release hole is slightly smaller than the radius of the device (i.e., $0.9\,\mathrm{R} \leq a_0 \leq \mathrm{R}$), Equation (39) becomes

$$\frac{\mathrm{M}(s)}{\mathrm{M}(\infty)} = \frac{2\,Sh\,a_0\,\sin\left(\frac{\sqrt{-s}\,H}{R}\right) R^2\,F_1\,\cos\left(\frac{\sqrt{-s-\alpha_{1,1}^2}\,H}{R}\right) J_1\left(\frac{\alpha_{1,1}\,a_0}{R}\right)s}{H(-s)^{(3/2)}\left(\sin\left(\frac{\sqrt{-s}\,H}{R}\right)\sqrt{-s}\,R^2 - Sh\,\cos\left(\frac{\sqrt{-s}\,H}{R}\right)a_0^2\right)\alpha_{1,1}} + \frac{\sin\left(\frac{\sqrt{-s}\,H}{R}\right) R\,Sh\,a_0^2}{H(-s)^{(3/2)}\left(\sin\left(\frac{\sqrt{-s}\,H}{R}\right)\sqrt{-s}\,R^2 - Sh\,\cos\left(\frac{\sqrt{-s}\,H}{R}\right)a_0^2\right)} \tag{58}$$

because only the first term of the series (i.e., $n = 1$) is required for sufficient accuracy when $a_0 = R(1-\varepsilon)$ and $\varepsilon < 0.1$. As a result, F_1 becomes

$$F_1 = \frac{f_1(s)}{f_2(s)} \tag{59}$$

after using Equations (23) and (24) where

$$f_1(s) = 2\,\alpha_{1,1}\,R^3\,\sqrt{-s}\,\sin\left(\frac{\sqrt{-s}\,H}{R}\right) Sh\,a_0\,J_1\left(\frac{\alpha_{1,1}\,a_0}{R}\right) \tag{59A}$$

and

$$\begin{aligned} f_2(s) = & \left(\sin\left(\frac{\sqrt{-s-\alpha_{1,1}^2}\,H}{R}\right)\sqrt{-s-\alpha_{1,1}^2}\,J_0(\alpha_{1,1})^2\,\alpha_{1,1}^2\,R^4\,\sin\left(\frac{\sqrt{-s}\,H}{R}\right)\sqrt{-s}\right. \\ & -\sin\left(\frac{\sqrt{-s-\alpha_{1,1}^2}\,H}{R}\right)\sqrt{-s-\alpha_{1,1}^2}\,J_0(\alpha_{1,1})^2\,\alpha_{1,1}^2\,R^2\,Sh\,\cos\left(\frac{\sqrt{-s}\,H}{R}\right)a_0^2 \\ & -4\,Sh^2\,a_0^2\,\cos\left(\frac{\sqrt{-s}\,H}{R}\right)J_1\left(\frac{\alpha_{1,1}\,a_0}{R}\right)^2\cos\left(\frac{\sqrt{-s-\alpha_{1,1}^2}\,H}{R}\right)R^2 \\ & -Sh\,\cos\left(\frac{\sqrt{-s-\alpha_{1,1}^2}\,H}{R}\right)a_0^2\,\alpha_{1,1}^2\,J_0\left(\frac{\alpha_{1,1}\,a_0}{R}\right)^2\sin\left(\frac{\sqrt{-s}\,H}{R}\right)\sqrt{-s}\,R^2 \\ & +Sh^2\,\cos\left(\frac{\sqrt{-s-\alpha_{1,1}^2}\,H}{R}\right)a_0^4\,\alpha_{1,1}^2\,J_0\left(\frac{\alpha_{1,1}\,a_0}{R}\right)^2\cos\left(\frac{\sqrt{-s}\,H}{R}\right) \\ & -Sh\,\cos\left(\frac{\sqrt{-s-\alpha_{1,1}^2}\,H}{R}\right)a_0^2\,\alpha_{1,1}^2\,J_1\left(\frac{\alpha_{1,1}\,a_0}{R}\right)^2\sin\left(\frac{\sqrt{-s}\,H}{R}\right)\sqrt{-s}\,R^2 \\ & \left.+Sh^2\,\cos\left(\frac{\sqrt{-s-\alpha_{1,1}^2}\,H}{R}\right)a_0^4\,\alpha_{1,1}^2\,J_1\left(\frac{\alpha_{1,1}\,a_0}{R}\right)^2\cos\left(\frac{\sqrt{-s}\,H}{R}\right)\right)s \end{aligned} \tag{59B}$$

The dimensionless effective time is given by (see the Appendix)

$$\tau_{eff} = \frac{P_1}{P_2} \tag{60}$$

Although Equation (60) appears computationally intensive and involves transcendental functions, it can be implemented using Maple. It is possible to study the effects of geometry and the Sherwood number on the time constant for drug delivery because the equation depends on three dimensionless parameters: Sh, H/R, and a_0/R. Assuming that Sh = 100, the time constant increases with H/R (Figure 5). Similarly, when H/R = 2 and a_0/R = 0.9, Figure 6 shows that τ_{eff} decreases with any increase in the Sherwood number. As the resistance to mass transfer decreases (e.g., high mixing), the API is released at a faster rate. Poor mixing near the target site may severely affect the performance of the product. This point was also made in the case of an implant near a target tissue (Tojo and Miyanami, 1983).

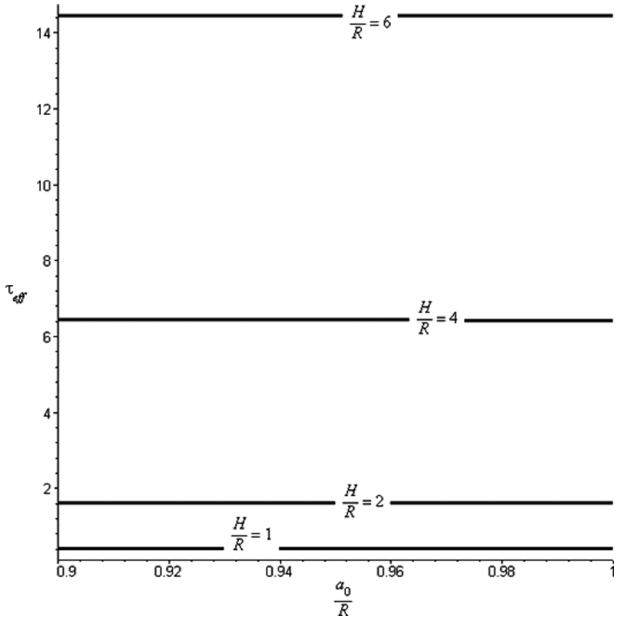

Figure 5. Effects of device geometry on the effective dimensionless time constant for $Sh = 100$.

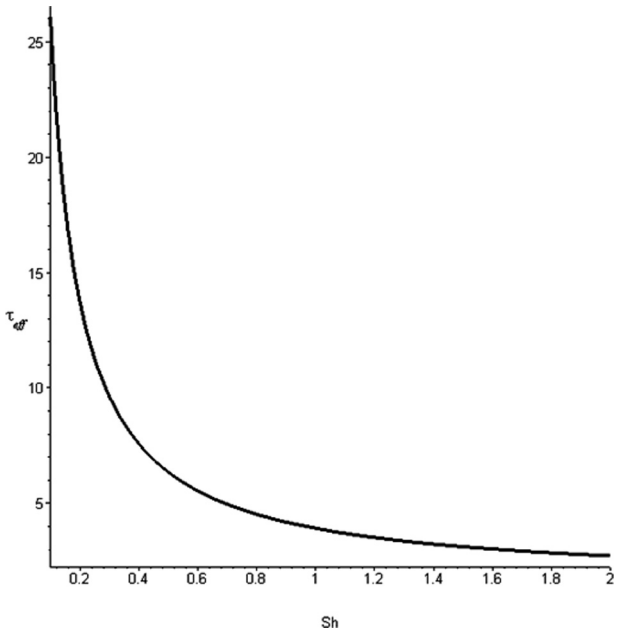

Figure 6. Relationship between the Sherwood number and the effective dimensionless time constant when $H/R = 2$ and $a_0/R = 0.9$.

General Case: The Release Hole is Smaller Than the Device Diameter ($0 < a_0 \leq R$)

When $0 < a_0 \leq \mathrm{R}$, Equation (39) is written as

$$\begin{aligned}\frac{\mathrm{M}(s)}{\mathrm{M}(\infty)} = &-\frac{2\,Sh\,a_0\,\sin\left(\frac{\sqrt{-s}\,H}{R}\right)R^2\,s\,F_1\,\cos\left(\frac{\sqrt{-s-\alpha_{1,1}^2}\,H}{R}\right)J_1\left(\frac{\alpha_{1,1}\,a_0}{R}\right)}{H(-s)^{(3/2)}\left(-\sin\left(\frac{\sqrt{-s}\,H}{R}\right)\sqrt{-s}\,R^2+Sh\,\cos\left(\frac{\sqrt{-s}\,H}{R}\right)a_0^2\right)\alpha_{1,1}}\\ &-\frac{2\,Sh\,a_0\,\sin\left(\frac{\sqrt{-s}\,H}{R}\right)R^2\,s\,F_2\,\cos\left(\frac{\sqrt{-s-\alpha_{1,2}^2}\,H}{R}\right)J_1\left(\frac{\alpha_{1,2}\,a_0}{R}\right)}{H(-s)^{(3/2)}\left(-\sin\left(\frac{\sqrt{-s}\,H}{R}\right)\sqrt{-s}\,R^2+Sh\,\cos\left(\frac{\sqrt{-s}\,H}{R}\right)a_0^2\right)\alpha_{1,2}}\\ &-\frac{Sh\,a_0^2\sin\left(\frac{\sqrt{-s}\,H}{R}\right)R}{H(-s)^{(3/2)}\left(-\sin\left(\frac{\sqrt{-s}\,H}{R}\right)\sqrt{-s}\,R^2+Sh\,\cos\left(\frac{\sqrt{-s}\,H}{R}\right)a_0^2\right)}\end{aligned} \tag{61}$$

because two terms of the series (i.e., $n = 2$) are sufficient. As a result, F_1 and F_2 are determined from Equations (23) and (24):

$$\begin{aligned}&-\frac{1}{2}F_1\,\sin\left(\frac{\sqrt{-s-\alpha_{1,1}^2}\,H}{R}\right)\sqrt{-s-\alpha_{1,1}^2}\,J_0(\alpha_{1,1})^2\\ &=\frac{2\,Sh^2\,a_0^2\,\cos\left(\frac{\sqrt{-s}\,H}{R}\right)J_1\left(\frac{\alpha_{1,1}\,a_0}{R}\right)^2F_1\,\cos\left(\frac{\sqrt{-s-\alpha_{1,1}^2}\,H}{R}\right)}{\left(-\sin\left(\frac{\sqrt{-s}\,H}{R}\right)\sqrt{-s}\,R^2+Sh\,\cos\left(\frac{\sqrt{-s}\,H}{R}\right)a_0^2\right)\alpha_{1,1}^2}\\ &+\frac{2\,Sh^2\,a_0^2\,\cos\left(\frac{\sqrt{-s}\,H}{R}\right)J_1\left(\frac{\alpha_{1,1}\,a_0}{R}\right)F_2\,\cos\left(\frac{\sqrt{-s-\alpha_{1,2}^2}\,H}{R}\right)J_1\left(\frac{\alpha_{1,2}\,a_0}{R}\right)}{\left(-\sin\left(\frac{\sqrt{-s}\,H}{R}\right)\sqrt{-s}\,R^2+Sh\,\cos\left(\frac{\sqrt{-s}\,H}{R}\right)a_0^2\right)\alpha_{1,1}\,\alpha_{1,2}}\\ &+\frac{Sh^2\,a_0^3\,\cos\left(\frac{\sqrt{-s}\,H}{R}\right)J_1\left(\frac{\alpha_{1,1}\,a_0}{R}\right)}{s\left(-\sin\left(\frac{\sqrt{-s}\,H}{R}\right)\sqrt{-s}\,R^2+Sh\,\cos\left(\frac{\sqrt{-s}\,H}{R}\right)a_0^2\right)\alpha_{1,1}\,R}\\ &-\frac{1}{2}\frac{Sh\,F_1\,\cos\left(\frac{\sqrt{-s-\alpha_{1,1}^2}\,H}{R}\right)a_0\left(\frac{\sqrt{\pi}\,\alpha_{1,1}\,a_0\,J_0\left(\frac{\alpha_{1,1}\,a_0}{R}\right)^2}{R}+\frac{\sqrt{\pi}\,\alpha_{1,1}\,a_0\,J_1\left(\frac{\alpha_{1,1}\,a_0}{R}\right)^2}{R}\right)}{\sqrt{\pi}\,R\,\alpha_{1,1}}\\ &+Sh\,F_2\,\cos\left(\frac{\sqrt{-s-\alpha_{1,2}^2}\,H}{R}\right)a_0\left(J_1\left(\frac{\alpha_{1,2}\,a_0}{R}\right)\alpha_{1,2}\,J_0\left(\frac{\alpha_{1,1}\,a_0}{R}\right)\right.\\ &\left.-J_0\left(\frac{\alpha_{1,2}\,a_0}{R}\right)J_1\left(\frac{\alpha_{1,1}\,a_0}{R}\right)\alpha_{1,1}\right)/(R(\alpha_{1,1}^2-\alpha_{1,2}^2))-\frac{Sh\,a_0\,J_1\left(\frac{\alpha_{1,1}\,a_0}{R}\right)}{s\,\alpha_{1,1}\,R}\end{aligned} \tag{62}$$

and

$$
\begin{aligned}
&-\frac{1}{2}F_2 \sin\left(\frac{\sqrt{-s-\alpha_{1,2}^2}H}{R}\right)\sqrt{-s-\alpha_{1,2}^2}J_0(\alpha_{1,2})^2 = \\
&\frac{2\,Sh^2 a_0^2 \cos\left(\frac{\sqrt{-s}H}{R}\right)J_1\left(\frac{\alpha_{1,2}a_0}{R}\right)F_1 \cos\left(\frac{\sqrt{-s-\alpha_{1,1}^2}H}{R}\right)J_1\left(\frac{\alpha_{1,1}a_0}{R}\right)}{\left(-\sin\left(\frac{\sqrt{-s}H}{R}\right)\sqrt{-s}\,R^2 + Sh\,\cos\left(\frac{\sqrt{-s}H}{R}\right)a_0^2\right)\alpha_{1,2}\alpha_{1,1}} \\
&+\frac{2\,Sh^2 a_0^2 \cos\left(\frac{\sqrt{-s}H}{R}\right)J_1\left(\frac{\alpha_{1,2}a_0}{R}\right)^2 F_2 \cos\left(\frac{\sqrt{-s-\alpha_{1,2}^2}H}{R}\right)}{\left(-\sin\left(\frac{\sqrt{-s}H}{R}\right)\sqrt{-s}\,R^2 + Sh\,\cos\left(\frac{\sqrt{-s}H}{R}\right)a_0^2\right)\alpha_{1,2}^2} \\
&+\frac{Sh^2 a_0^3 \cos\left(\frac{\sqrt{-s}H}{R}\right)J_1\left(\frac{\alpha_{1,2}a_0}{R}\right)}{s\left(-\sin\left(\frac{\sqrt{-s}H}{R}\right)\sqrt{-s}\,R^2 + Sh\,\cos\left(\frac{\sqrt{-s}H}{R}\right)a_0^2\right)\alpha_{1,2}R} + Sh\,F_1 \cos\left(\frac{\sqrt{-s-\alpha_{1,1}^2}H}{R}\right)a_0 \\
&\left(J_1\left(\frac{\alpha_{1,2}a_0}{R}\right)\alpha_{1,2}J_0\left(\frac{\alpha_{1,1}a_0}{R}\right) - J_0\left(\frac{\alpha_{1,2}a_0}{R}\right)J_1\left(\frac{\alpha_{1,1}a_0}{R}\right)\alpha_{1,1}\right)\Big/\left(R(\alpha_{1,1}^2-\alpha_{1,2}^2)\right) \\
&-\frac{1}{2}\frac{Sh\,F_2 \cos\left(\frac{\sqrt{-s-\alpha_{1,2}^2}H}{R}\right)a_0\left(\frac{\sqrt{\pi}\alpha_{1,2}a_0 J_0\left(\frac{\alpha_{1,2}a_0}{R}\right)^2}{R} + \frac{\sqrt{\pi}\alpha_{1,2}a_0 J_1\left(\frac{\alpha_{1,2}a_0}{R}\right)^2}{R}\right)}{\sqrt{\pi}\,R\,\alpha_{1,2}} \\
&-\frac{Sh\,a_0 J_1\left(\frac{\alpha_{1,2}a_0}{R}\right)}{s\,\alpha_{1,2}R}
\end{aligned}
\tag{63}
$$

It may be necessary to increase the number of terms in the series to achieve convergence if the hole is very small relative to the device diameter. Equations (41)–(43) can be analyzed using computer algebra software. The case when the Sherwood number tends to infinity is considered. The following equations are obtained:

$$\frac{\mathrm{M}(s)}{\mathrm{M}(\infty)} = -\frac{\sin\left(\frac{\sqrt{-s}H}{R}\right)R}{\cos\left(\frac{\sqrt{-s}H}{R}\right)(-s)^{(3/2)}H} \tag{64}$$

and

$$\tau_{eff} = \frac{2H^2}{5R^2} \tag{65}$$

The effective dimensionless time constant is not a function of a_0. In addition, the inverse Laplace transform for Equation (64) is

$$\frac{\mathrm{M}(\tau)}{\mathrm{M}(\infty)} = 1 - \left(\sum_{q=0}^{\infty}\left(\frac{8\,\mathrm{e}^{\left(-\frac{(2q+1)^2\pi^2\tau}{4\gamma^2}\right)}}{\pi^2(2q+1)^2}\right)\right) \tag{66}$$

where

$$\chi = \frac{H}{R} \tag{67}$$

Figure 7 is obtained using Equation (66) with different values of the aspect ratio χ. The effect of χ on τ_{eff} is better captured in Figure 8:

$$\tau_{eff} = \frac{2\chi^2}{5} \tag{68}$$

Note that for practical purposes, the following equation, obtained when $q = 0$, can be used to estimate $M(\tau)/M(\infty)$as a first-order process:

$$\frac{M(\tau)}{M(\infty)} \approx 1 - \frac{8}{\pi^2} e^{-\left(\frac{\pi^2}{10}\right)\frac{\tau}{\tau_{eff}}} \approx 1 - 0.81 e^{-\frac{\tau}{\tau_{eff}}} \tag{69}$$

Figure 9 shows how τ_{eff} is affected by χ for different values of a_0/R, after using Equations (43), (62) and (63), when the Sherwood number is large but finite (e.g., $Sh = 100$). The trend observed in Figure 5 is repeated: τ_{eff} decreases with an increase in the diameter and its value rises with an increase in H.

Figure 10 shows the release of benzoic acid through a small hole centered at the top surface of three cylindrical devices coated with a sealed polymethyl methacrylate (PMMA) layer (Tojo and Miyanami, 1983). The drug was saturated in 1% (w/w) agar solution and diffusion occurred only through this solution and not through the mold itself. All of the parameter values, including R, H, and a_0, were obtained from Tojo and Miyanami (1983). The radius and height of the designs were 0.4 cm

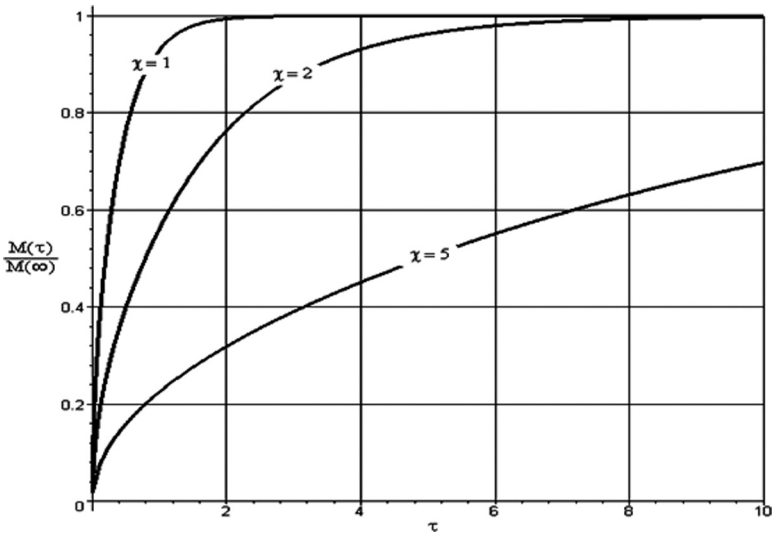

Figure 7. Effects of the aspect ratio $\chi = H/R$ on the cumulative amount of drug released when $0 < a_0 \leq$ R and when the Sherwood number approaches infinity.

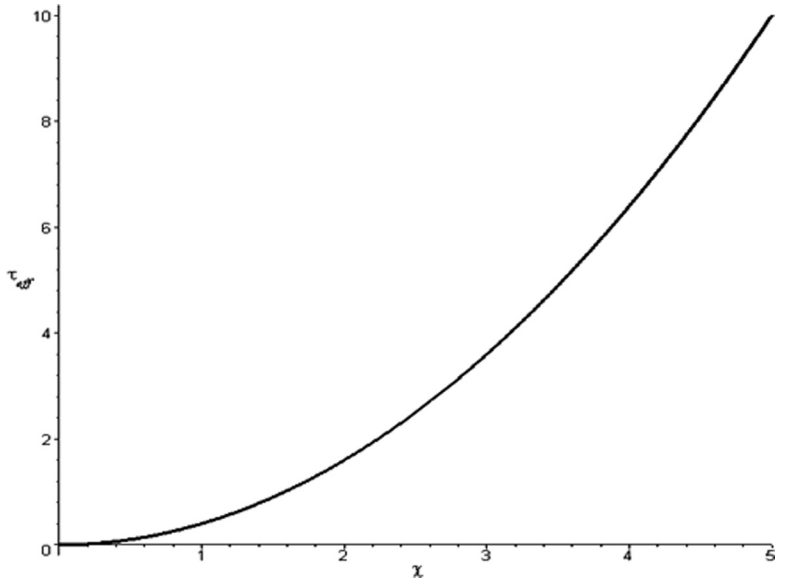

Figure 8. Effects of the aspect ratio $\chi = H/R$ on the effective dimensionless time constant when $0 < a_0 \leq \mathrm{R}$ and when the Sherwood number approaches infinity.

and 1.6 cm, respectively. Differences were noted in the radius of the release hole, which ranged from 0.1 to 0.4 cm. A 300 mL beaker holding deionized water was used for the experiments. Except when $a_0/R = 1$, the analytical solution predicts the laboratory data very well and is also in agreement with the numerical results presented

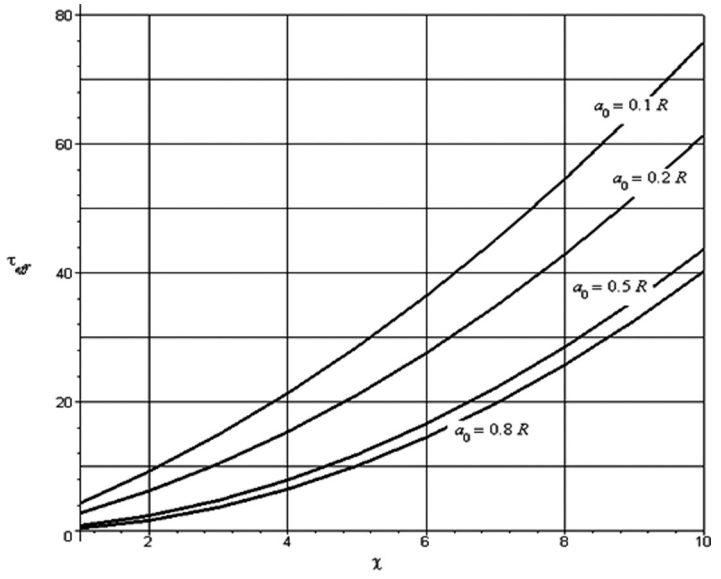

Figure 9. Influences of a_0/R and the aspect ratio $\chi = H/R$ on the effective dimensionless time constant when $0 < a_0 \leq \mathrm{R}$ and when $Sh = 100$.

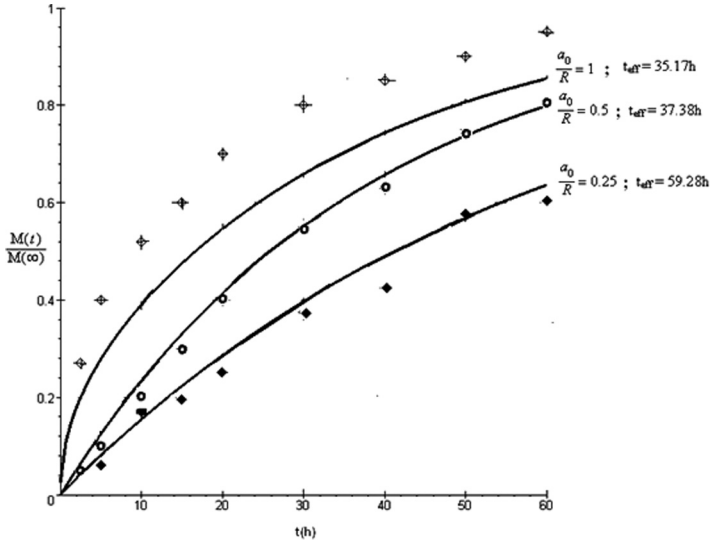

Figure 10. Predicted (—) and experimental cumulative amount of benzoic acid released for various a_0/R values. The time constants, calculated from Equation (43) and $t_{eff} = \frac{R^2\tau_{eff}}{\eta_A}$, are shown.

in Tojo and Miyanami (1983) (profile not shown). The coefficients of determination are 0.95, 0.96, and 0.72 for $a_0/R = 0.25$, 0.5, and 1, respectively. The large deviation observed when $a_0/R = 1$ may be due to an initial burst release of the drug (Tojo, 1984). In addition, the time constant is reduced with an increase in a_0. The following data were used in the study: $\eta_A = 8.1 \times 10^{-6}\text{cm}^2/\text{s}$ and $k_m = 0.005$ cm/s. Procedures for estimating η_A and k_m were outlined in Tojo (1984). The parameter η_A was calculated based on the diffusivity of benzoic acid in pure water and the mass percentage of anhydrous agar in the gel. The mass transfer coefficient was determined from the dissolution of benzoic acid in water (Tojo, 1984).

The cases studied in this work have wide applications in controlled-released technology and the approach can be extended to other cylindrical systems, as well. The main differences would stem from the boundary conditions. The methodology described can be combined with a pharmacokinetic model to investigate the time required to reach a target drug concentration in the blood. Design specifications are directly linked to the plasma profile of the API, and the therapeutic drug levels can be managed with greater control and accuracy.

Conclusions

An analytical and computational study of a cylindrical system with a circular release hole was conducted for controlled drug delivery. Expressions for the time constant and the cumulative amount of drug released were provided for three cases that differed by the dimension of a release hole relative to the product diameter. The transient two-dimensional model was studied using Laplace transform techniques, the Bromwich integral, and the residue theorem. When the release hole and the cylinder were of equal diameters, the total amount of drug delivered was an

increasing function of the mass transfer and diffusion coefficient and a decreasing function of the device length. The release rate increases with the mass transfer coefficient. A similar conclusion was reached when the radius of the opening was marginally smaller than that of the system. However, the expressions obtained in this case were computationally demanding when compared to the equal-radius design specifications. The last case study showed that the methodology was well suited for any size requirement but involved more elaborate calculations. A potential application of the method is the prediction of the time it takes to reach a desired plasma concentration.

References

Alexis, F., Venkatraman, S. S., Rath, S. K., and Boey, F. (2004). In vitro study of release mechanisms of paclitaxel and rapamycin from drug-incorporated biodegradable stent matrices, *J. Control. Release*, **98**, 67–74.

Andresen, T., Upton, R. N., Foster, D. J. R., Christrup, L. L., Arendt-Nielsen, L., and Drewes, A. M. (2011). Pharmacokinetic/pharmacodynamic relationships of transdermal buprenorphine and fentanyl in experimental human pain models, *Basic Clin. Pharmacol. Toxicol.*, **108**, 274–284.

Collins, R. (1980). The choice of an effective time constant for diffusive processes in finite systems, *J. Phys. D Appl. Phys.*, **13**, 1935–1947.

Ertan, G., Karasulu, E., Demirtas, D., Arici, M., and Guneri, T. (1997). Release characteristics of implantable cylindrical polyethylene matrices, *J. Pharm. Pharmacol.*, **49**, 229–235.

Ertan, G., Özyazici, M., Karasulu, M., Arici, E., and Güneri, T. (2005). In vitro programmable implants for constant drug release, *Acta Pharm. Turc.*, **47**, 243–256.

Gupta, C., and Chauhan, A. (2001). Ophthalmic delivery of cyclosporine A by punctal plugs, *J. Control. Release*, **150**, 70–76.

Hsu, J. P., Ting, C., and Lin, M. J. (1992). A theoretical analysis of a new drug delivery system: Cylindrical device with a vertical opening on its surface, *J. Pharm. Sci.*, **81**, 866–870.

Kreye, F., Siepmann, F., and Siepmann, J. (2011). Drug release mechanisms of compressed lipid implants, *Int. J. Pharm.*, **404**, 27–35.

Leopold, A., Wilson, S., Weaver, J. S., and Moursi, A. M. (2002). Pharmacokinetics of lidocaine delivered from a transmucosal patch in children, *Anesth. Prog.*, **49**, 82–87.

Mystakidou, K., Tsilika, E., Tsiatas, M., and Vlahos, L. (2007). Oral transmucosal fentanyl citrate in cancer pain management: A practical application of nanotechnology, *Int. J. Nanomedicine*, **2**, 49–54.

Qian, F., Szymanski, A., and Gao, J. (2001). Fabrication and characterization of controlled release poly(D,L-lactide-co-glycolide) millirods, *J. Biomed. Mater. Res.*, **55**, 512–522.

Rosca, I., and Vergnaud, J. (2008). Evaluation of the characteristics of oral dosage forms with release controlled by erosion, *Comput. Biol. Med.*, **38**, 668–675.

Simon, L. (2011). A computational procedure for assessing the dynamic performance of diffusion-controlled transdermal delivery devices, *Pharmaceutics*, **3**, 485–496.

Tojo, K. (1984). Prolonged drug release from a simple cylindrical device with a small hole, *Chem. Eng. Commun.*, **30**, 311–322.

Tojo, K., and Miyanami, K. (1983). Controlled release from a cylindrical matrix device, *Bull. Osaka Prefect. Univ. Ser. A Eng. Nat. Sci.*, **31**, 149–157.

Wang, D. M., Lin, F. C., Chen, L. Y., and Lai. J. Y. (1998). Application of asymmetric TPX membranes to transdermal delivery of nitroglycerin, *J. Control. Release*, **50**, 187–195.

Appendix

Expression for τ_{eff} in Equation (60): $\tau_{eff} = P_1/P_2$

$$
\begin{aligned}
P_1 = \Bigg(& 4\,H^3\,Sh^3 a_0^6\,J_0\,(\alpha_{1,1})^2\,\alpha_{1,1}^5\,J_0\Big(\frac{\alpha_{1,1}\,a_0}{R}\Big)^2 R^2\,\cosh\Big(\frac{\alpha_{1,1}\,H}{R}\Big)\sinh\Big(\frac{\alpha_{1,1}\,H}{R}\Big) \\
& + 20\,R^5\,Sh^2\,a_0^4\,\sinh\Big(\frac{\alpha_{1,1}\,H}{R}\Big)J_0(\alpha_{1,1})^2\,\alpha_{1,1}^5\,H^2\,\cosh\Big(\frac{\alpha_{1,1}\,H}{R}\Big)J_1\Big(\frac{\alpha_{1,1}\,a_0}{R}\Big)^2 \\
& + 30\,H\,R^8\,Sh\,a_0^2\,\sinh\Big(\frac{\alpha_{1,1}\,H}{R}\Big)J_0(\alpha_{1,1})^2\,\alpha_{1,1}^5\,\cosh\Big(\frac{\alpha_{1,1}\,H}{R}\Big)J_0\Big(\frac{\alpha_{1,1}\,a_0}{R}\Big)^2 \\
& + 20\,R^5\,Sh^2\,a_0^4\,\sinh\Big(\frac{\alpha_{1,1}\,H}{R}\Big)J_0(\alpha_{1,1})^2\,\alpha_{1,1}^5\,H^2\,\cosh\Big(\frac{\alpha_{1,1}\,H}{R}\Big)J_0\Big(\frac{\alpha_{1,1}\,a_0}{R}\Big)^2 \\
& + 4\,H^3\,Sh^3\,a_0^6\,J_0(\alpha_{1,1})^2\,\alpha_{1,1}^5\,J_1\Big(\frac{\alpha_{1,1}\,a_0}{R}\Big)^2 R^2\,\cosh\Big(\frac{\alpha_{1,1}\,H}{R}\Big)\sinh\Big(\frac{\alpha_{1,1}\,H}{R}\Big) \\
& - 40\,Sh^2\,a_0^2\,H^2\,R^7\,J_1\Big(\frac{\alpha_{1,1}\,a_0}{R}\Big)^2\cosh\Big(\frac{\alpha_{1,1}\,H}{R}\Big)\sinh\Big(\frac{\alpha_{1,1}\,H}{R}\Big)^2 J_0(\alpha_{1,1})^2\,\alpha_{1,1}^3 \\
& - 16\,H^3\,R^4\,Sh^3\,a_0^4\,J_0(\alpha_{1,1})^2\,\alpha_{1,1}^3\,J_1\Big(\frac{\alpha_{1,1}\,a_0}{R}\Big)^2\cosh\Big(\frac{\alpha_{1,1}\,H}{R}\Big)\,\sinh\Big(\frac{\alpha_{1,1}\,H}{R}\Big) \\
& + 30\,H\,R^8 Sh\,a_0^2\,\sinh\Big(\frac{\alpha_{1,1}\,H}{R}\Big)^2 J_0(\alpha_{1,1})^2\,\alpha_{1,1}^5\,\cosh\Big(\frac{\alpha_{1,1}\,H}{R}\Big)\,J_1\Big(\frac{\alpha_{1,1}\,a_0}{R}\Big)^2 \\
& + 10\,H^2\,Sh^3\,a_0^6\,\alpha_{1,1}^4\,\cosh\Big(\frac{\alpha_{1,1}\,H}{R}\Big)^2 J_1\Big(\frac{\alpha_{1,1}\,a_0}{R}\Big)^4 R^3 \\
& + 15\,H\,R^6\,Sh^2\,a_0^4\,\alpha_{1,1}^4\,\cosh\Big(\frac{\alpha_{1,1}\,H}{R}\Big)^2 J_0\Big(\frac{\alpha_{1,1}\,a_0}{R}\Big)^4 \\
& + 30\,H\,R^6\,Sh^2\,a_0^4\,\alpha_{1,1}^4\,\cosh\Big(\frac{\alpha_{1,1}\,H}{R}\Big)^2 J_0\Big(\frac{\alpha_{1,1}\,a_0}{R}\Big)^2 J_1\Big(\frac{\alpha_{1,1}\,a_0}{R}\Big)^2 \\
& - 40\,Sh^3\,a_0^4\,H^2\,R^5 J_1\Big(\frac{\alpha_{1,1}\,a_0}{R}\Big)^2\cosh\Big(\frac{\alpha_{1,1}\,H}{R}\Big)\,\alpha_{1,1}^2\,J_0\Big(\frac{\alpha_{1,1}\,a_0}{R}\Big)^2 \\
& - 16\,\alpha_{1,1}^2\,H^3\,Sh^4\,a_0^6\,J_1\Big(\frac{\alpha_{1,1}\,a_0}{R}\Big)^2 J_0\Big(\frac{\alpha_{1,1}\,a_0}{R}\Big)^2 R^2\cosh\Big(\frac{\alpha_{1,1}\,H}{R}\Big)^2 \\
& + 30\,Sh^2\,a_0^2\,R^9 J_1\Big(\frac{\alpha_{1,1}\,a_0}{R}\Big)^2\cosh\Big(\frac{\alpha_{1,1}\,H}{R}\Big)\,\sinh\Big(\frac{\alpha_{1,1}\,H}{R}\Big)J_0(\alpha_{1,1})^2\,\alpha_{1,1} \\
& + 20\,H^2\,Sh^3\,a_0^6\,\alpha_{1,1}^4\,\cosh\Big(\frac{\alpha_{1,1}\,H}{R}\Big)^2 J_0\Big(\frac{\alpha_{1,1}\,a_0}{R}\Big)^2 J_1\Big(\frac{\alpha_{1,1}\,a_0}{R}\Big)^2\,R_3 \\
& + 15\,\alpha_{1,1}^6\,H\,R^{10}\,J_0(\alpha_{1,1})^4\,\cosh\Big(\frac{\alpha_{1,1}\,H}{R}\Big)^2 - 10\,R^7\,Sh\,a_0^2\,\alpha_{1,1}^6\,J_0(\alpha_{1,1})^4\,H^2 \\
& - 2\,H^3\,Sh^2\,a_0^4\,\alpha_{1,\,1}^6 J_0(\alpha_{1,1})^4\,R^4 + 2\,H^3\,Sh^4\,a_0^8\,\alpha_{1,1}^4\cosh\Big(\frac{\alpha_{1,1}\,H}{R}\Big)^2 \\
& J_0\Big(\frac{\alpha_{1,1}\,a_0}{R}\Big)^4 + 2\,H^3\,Sh^4\,a_0^8\,\alpha_{1,1}^4\,\cosh\Big(\frac{\alpha_{1,1}\,H}{R}\Big)^2 J_1\Big(\frac{\alpha_{1,1}\,a_0}{R}\Big)^4
\end{aligned}
$$

$$
\begin{aligned}
&- 15\,\alpha_{1,1}^6\,H\,J_0(\alpha_{1,1})^4\,R^{10} - 40\,Sh^3\,a_0^4\,H^2\,R^5 J_1\left(\frac{\alpha_{1,1}\,a_0}{R}\right)^4 \\
&\cosh\left(\frac{\alpha_{1,1}\,H}{R}\right)^2\,\alpha_{1,1}^2 + 10\,H^2\,Sh^3\,a_0^6\,\alpha_{1,1}^4\,\cosh\left(\frac{\alpha_{1,1}\,H}{R}\right)^2 J_0\left(\frac{\alpha_{1,1}\,a_0}{R}\right) R_3 \\
&+ 4\,H^3\,Sh^4\,a_0^8\,\alpha_{1,1}^4\,J_0\left(\frac{\alpha_{1,1}\,a_0}{R}\right)^2 J_1\left(\frac{\alpha_{1,1}\,a_0}{R}\right)^2 \cosh\left(\frac{\alpha_{1,1}\,H}{R}\right)^2 \\
&+ 2\,H^3\,R^4\,Sh^2\,a_0^4\,\alpha_{1,1}^6\,J_0(\alpha_{1,1})^4\,\cosh\left(\frac{\alpha_{1,1}\,H}{R}\right)^2 \\
&+ 10\,R^7\,Sh\,a_0^2\,\alpha_{1,1}^6\,J_0(\alpha_{1,1})^4\,\cosh\left(\frac{\alpha_{1,1}\,H}{R}\right)^2 H^2 \\
&+ 30\,Sh^2\,a_0^2\,R^8\,J_1\left(\frac{\alpha_{1,1}\,a_0}{R}\right)^2 H\,\alpha_{1,1}^2\,J_0(\alpha_{1,1})^2 \\
&+ 15\,Sh^2\,a_0^4\,\alpha_{1,1}^4\,H\,\cosh\left(\frac{\alpha_{1,1}\,H}{R}\right)^2 J_1\left(\frac{\alpha_{1,1}\,a_0}{R}\right)^4 R_6 \\
&- 16\,\alpha_{1,1}^2\,H^3\,Sh^4\,a_0^6\,J_1\left(\frac{\alpha_{1,1}\,a_0}{R}\right)^4 R^2 \cosh\left(\frac{\alpha_{1,1}\,H}{R}\right)^2 \\
&+32\,Sh^4\,a_0^4\,H^3\,J_1\left(\frac{\alpha_{1,1}\,a_0}{R}\right)^4 R^4 \cosh\left(\frac{\alpha_{1,1}\,H}{R}\right)^2\Bigg) \\
&\left(Sh\,a_0^2\cosh\left(\frac{\alpha_{1,1}\,H}{R}\right)\alpha_{1,1}^2\,J_0\left(\frac{\alpha_{1,1}\,a_0}{R}\right)^2 + \sinh\left(\frac{\alpha_{1,1}\,H}{R}\right)\alpha_{1,1}^3\,J_0(\alpha_{1,1})^2\,R_2\right. \\
&\left.+\,Sh\,a_0^2\cosh\left(\frac{\alpha_{1,1}\,H}{R}\right)\alpha_{1,1}^2\,J_1\left(\frac{\alpha_{1,1}\,a_0}{R}\right)^2 - 4\,Sh\,J_1\left(\frac{\alpha_{1,1}\,a_0}{R}\right)^2\cosh\left(\frac{\alpha_{1,1}\,H}{R}\right)R^2\right)
\end{aligned}
$$

$$
\begin{aligned}
P_2 = {} & 5\;Sh\,a_0^2\,R^2\left(2\,Sh\,a_0^2\;\sinh\left(\frac{\alpha_{1,1}\,H}{R}\right)J_0(\alpha_{1,1})^2\alpha_{1,1}^5\,R^2\cosh\left(\frac{\alpha_{1,1}\,H}{R}\right)\right. \\
& J_0\left(\frac{\alpha_{1,1}\,a_0}{R}\right)^2 + Sh^2\,a_0^4\,\alpha_{1,1}^4\,\cosh\left(\frac{\alpha_{1,1}\,H}{R}\right)^2 J_1\left(\frac{\alpha_{1,1}\,a_0}{R}\right)^4 \\
& - 8\,Sh^2\,a_0^2\,\alpha_{1,1}^2\;J_1\left(\frac{\alpha_{1,1}\,a_0}{R}\right)^2\cosh\left(\frac{\alpha_{1,1}\,H}{R}\right)^2 R^2\,J_0\left(\frac{\alpha_{1,1}\,a_0}{R}\right)^2 \\
& - \alpha_{1,1}^6 J_0(\alpha_{1,1})^4\,R^4 + 2\,Sh\,a_0^2\;\sinh\left(\frac{\alpha_{1,1}\,H}{R}\right)J_0\,(\alpha_{1,1})^2\,\alpha_{1,1}^5\,R^2 \\
& \cosh\left(\frac{\alpha_{1,1}\,H}{R}\right)J_1\left(\frac{\alpha_{1,1}\,a_0}{R}\right)^2 + 16\,Sh^2\,J_1\left(\frac{\alpha_{1,1}\,a_0}{R}\right)^4\cosh\left(\frac{\alpha_{1,1}\,H}{R}\right)^2 R^4 \\
& + \alpha_{1,1}^6\,J_0(\alpha_{1,1})^4\,R^4\cosh\left(\frac{\alpha_{1,1}\,H}{R}\right)^2 \\
& - 8\,Sh^2\,a_0^2\,\alpha_{1,1}^2\,J_1\left(\frac{\alpha_{1,1}\,a_0}{R}\right)^4\cosh\left(\frac{\alpha_{1,1}\,H}{R}\right)^2 R^2
\end{aligned}
$$

$$
\begin{aligned}
&+ Sh^2\, a_0^4\, \alpha_{1,1}^4\, \cosh\left(\frac{\alpha_{1,1}\, H}{R}\right)^2 J_0\left(\frac{\alpha_{1,1}\, a_0}{R}\right)^4 \\
&+ 2Sh^2\, a_0^4\, \alpha_{1,1}^4 \cosh\left(\frac{\alpha_{1,1}\, H}{R}\right)^2 J_0\left(\frac{\alpha_{1,1}\, a_0}{R}\right)^2 J_1\left(\frac{\alpha_{1,1}\, a_0}{R}\right)^2 \\
&-8\, Sh\, \sinh\left(\frac{\alpha_{1,1}\, H}{R}\right) J_0(\alpha_{1,1})^2\, \alpha_{1,1}^3\, R^4\, J_1\left(\frac{\alpha_{1,1}\, a_0}{R}\right)^2 \cosh\left(\frac{\alpha_{1,1}\, H}{R}\right)\Bigg) \\
&\Bigg(H\, Sh^2\, a_0^4 \cosh\left(\frac{\alpha_{1,1}\, H}{R}\right) \alpha_{1,1}^2\, J_0\left(\frac{\alpha_{1,1}\, a_0}{R}\right)^2 \\
&+ H\, Sh^2\, a_0^4 \cosh\left(\frac{\alpha_{1,1}\, H}{R}\right) \alpha_{1,1}^2\, J_1\left(\frac{\alpha_{1,1}\, a_0}{R}\right)^2 \\
&+ 3\, R^5\, \sinh\left(\frac{\alpha_{1,1}\, H}{R}\right) \alpha_{1,1}^3\, J_0(\alpha_{1,1})^2 \\
&+ 3\, R^3\, Sh\, a_0^2 \cosh\left(\frac{\alpha_{1,1}\, H}{R}\right) \alpha_{1,1}^2\, J_1\left(\frac{\alpha_{1,1}\, a_0}{R}\right)^2 \\
&+ Sh\, a_0^2 \sinh\left(\frac{\alpha_{1,1}\, H}{R}\right) \alpha_{1,1}^3\, H\, J_0(\alpha_{1,1})^2\, R^2 \\
&- 4\, H\, Sh^2\, a_0^2\, J_1\left(\frac{\alpha_{1,1}\, a_0}{R}\right)^2 \cosh\left(\frac{\alpha_{1,1}\, H}{R}\right) R^2 \\
&+3\, R^3\, Sh\, a_0^2 \cosh\left(\frac{\alpha_{1,1}\, H}{R}\right) \alpha_{1,1}^2\, J_0\left(\frac{\alpha_{1,1}\, H}{R}\right)^2\Bigg)
\end{aligned}
$$